JOURNAL OF PROPULSION AND POWER
Vol. 15, No. 6, November–December 1999

Mechanism of Combustion Instability in a Lean Premixed Dump Combustor

K. K. Venkataraman,* L. H. Preston,† D. W. Simons,† B. J. Lee,‡ J. G. Lee,§ and D. A. Santavicca¶
Pennsylvania State University, University Park, Pennsylvania 16802

Results from an experimental study of the mechanism of unstable combustion in a coaxial, optically accessible, bluff-body-stabilized dump combustor with natural gas as the fuel are reported. A parametric study was performed to investigate the effects of equivalence ratio, inlet velocity, inlet fuel distribution, inlet swirl, and centerbody recess on combustion stability. It was found that all of these parameters had an effect on the stability characteristics of this combustor. At selected unstable operating conditions, phase-resolved CH chemiluminescence images were captured to study the heat-release structure during one period of pressure oscillation. The flame–flowfield interaction that is depicted in these images indicates that flame–vortex interactions, and the resultant flame area changes, play a significant role in the instabilities that occur when there is no swirl. A simple analysis of these images, however, showed that fluctuating flame area and equivalence ratio fluctuations both contribute to the heat release fluctuations that drive the instability. Unstable combustion with swirl appears to be fundamentally different from unstable combustion without swirl in that instabilities with swirl occur near lean blowout and appear to be associated with repeated detaching and reattaching of the flame from the centerbody.

Introduction

STRINGENT emission standards have been codified to limit NO_x emissions from gas turbine engines, and with energy demands continually rising, these standards can only be expected to tighten. Conventional combustors rely on diffusion flames that burn at near-stoichiometric conditions causing high flame temperatures that result in unacceptable levels of thermal NO_x. Strategies to reduce NO_x levels have tried to reduce the flame temperature in the combustion zone by altering the fuel distribution in the primary zone or changing the chemistry of the flame by using a catalyst. The three main methods of changing the primary zone fuel distribution are based on the rich-burn/quick-quench/lean-burn,[1] lean premixed prevaporized (LPP), and lean direct injection[2] strategies. Of these, LPP combustion is generally agreed to hold the greatest promise for NO_x control.[3]

In the LPP concept, a homogenous lean fuel–air mixture is delivered to the primary zone, and combustion occurs at lower temperatures as the fuel burns at leaner equivalence ratios. Whereas this mode of operation is successful in reducing NO_x levels, it is extremely susceptible to combustion instability in the form of combustion-induced pressure oscillations. This is a resonance phenomenon associated with the acoustic characteristics of the combustor and is accompanied by high noise levels and severe pressure oscillations that can cause structural damage to engine components. The viability of the LPP combustion concept hinges on successful control of unstable combustion.

Received 5 November 1998; revision received 24 August 1999; accepted for publication 27 August 1999.

*Research Assistant, Propulsion Engineering Research Center, Department of Mechanical Engineering, 13 Research Building East, Bigler Road.

†Research Assistant, Department of Mechanical Engineering; currently Engineer, M/S 717-91, Large Military Engines Division, Pratt and Whitney, United Technologies Corporation, P.O. Box 109600, West Palm Beach, FL 33410.

‡Research Associate, Propulsion Engineering Research Center, Department of Mechanical Engineering; currently Assistant Professor, Department of Mechanical Engineering, Yeungnam University, Daedong, Kyoungsan, Gyoungbuk, 712-749 Korea.

§Research Associate, Propulsion Engineering Research Center, Department of Mechanical Engineering, 135 Research Building East, Bigler Road.

¶Professor, Propulsion Engineering Research Center, Department of Mechanical Engineering, 132 Research Building East, Bigler Road.

Four modes of unstable combustion can occur in gas turbine combustors: bulk, longitudinal, circumferential, and transverse modes.[4,5] A bulk-mode instability is an instability where the pressure inside the combustor varies temporally but not spatially. The frequency associated with this instability mode is the Helmholtz frequency of the acoustic system and is typically less than several hundred hertz. The important parameter involved is the volume of the combustor rather than any single dimension. A longitudinal-mode instability is one where a longitudinal acoustic wave is amplified within the combustor. The characteristic dimension for calculating the frequency of a longitudinal-mode instability is the acoustic length of the combustor. The frequencies of longitudinal modes are typically greater than several hundred hertz but less than a kilohertz. Such instabilities are often referred to as rumble. Circumferential-mode instabilities occur in annular combustors where the characteristic dimension is the circumference of the annular combustion chamber. Circumferential-mode frequencies are typically in the same range as longitudinal-mode instabilities. In the case of transverse-mode instabilities, the characteristic dimension is the radius of the combustor resulting in frequencies typically greater than 1 kHz. Transverse-mode instabilities are often referred to as screech, because of the higher frequencies of the pressure oscillations, and are most often encountered in afterburners. In this study, longitudinal pressure oscillations are set up inside the combustor and examined in detail.

It has long been known that unstable combustion is characterized by periodic heat-release and pressure oscillations. Rayleigh[6] postulated that, for the pressure oscillations to be amplified, the heat-release and pressure oscillations must be in phase; however, the exact mechanism of unstable combustion is still not completely understood. Before discussing the current state of knowledge of the mechanism of unstable combustion, the terminology used to describe such phenomena needs to be defined. One important distinction that needs to be made is between processes associated with the initiation of unstable combustion and processes associated with sustaining unstable combustion. Most studies to date, including this one, have focused on the limit cycle behavior of unstable combustion, and therefore, it is the phenomena that sustain the instability that are of interest. In a limit cycle, where the concept of cause and effect is ambiguous, it is the feedback loop between pressure fluctuations and heat-release fluctuations that sustains the instability and that must be understood. In particular, it is the mechanism whereby pressure fluctuations result in heat-release fluctuations that is most poorly understood and that is addressed in this paper.

The bulk of the research to date has studied combustion instability in single-nozzle, dump combustors or bluff-body combustors as a simplified way to examine the underlying phenomenology of unstable combustion.[4,5,7–16] The most often studied mechanisms whereby pressure fluctuations result in heat release fluctuations are flame–vortex interactions and equivalence ratio fluctuations.

The role of flame–vortex interactions in unstable combustion has been studied experimentally by a number of researchers.[7–11] One of the first studies of this phenomena was conducted by Rogers and Marble[7] in a ramjet combustor. More recently, Yu et al.,[8] Smith and Zukoski,[9] Poinsot et al.,[10] and Schadow et al.[11] have also conducted studies in model ramjet combustors. From the observations made in these studies, it is clear that as the vortex passes through the flame front there is a marked change in the flame area that in turn contributes to a change in the overall heat release.

Recently, there has been considerable interest in the role of equivalence ratio fluctuations in unstable combustion,[17–19] often referred to as feed–system coupling. This concept dates back to the work of Putnam,[20] who showed that many industrial burner oscillations could be explained in terms of, and eliminated by modifying, the fuel time lag, that is, the time from injection of the fuel to its combustion. This has led to a number of control strategies based on controlling or counteracting equivalence-ratio fluctuations. One of the most common methods used is to change the location of the fuel injector, thereby altering the fuel time lag such that the resultant heat-release fluctuations are out of phase with the pressure wave that drives the equivalence ratio fluctuations in the first place. Although some success has been achieved with this approach, that instabilities have been observed in combustors that have been designed to have no equivalence ratio fluctuations indicates that flame–flowfield interactions must also be accounted for.

In 1998, Peracchio and Proscia[21] presented a nonlinear heat-release/acoustic model that was tested on a single-nozzle rig. They considered both equivalence ratio fluctuations and flame area fluctuations as sources of heat-release fluctuations. The mean flame shape was calculated for a steady Poiseuille flow with imposed velocity perturbations. The flame dynamics model proposed by Fleifil et al.[22] was used to describe the response of the flame front to acoustic velocity perturbations. The effect of equivalence ratio fluctuations on heat release was calculated using time-lag concepts. The model required determination of a number of parameters that were calculated using pressure data from the single-nozzle rig. The model's performance was verified by checking for satisfactory agreement between heat-release data predicted by the model and those measured in the experiment. This work is important because the effects of both equivalence ratio variation and flame area variation were considered simultaneously. However, the parameter selection was such that the portion of the heat release attributed to flame area fluctuations was small compared to that due to fuel–air ratio variations. The authors acknowledge that the flame area fluctuations observed in other rigs were larger than those predicted by their model. Moreover, the model, with the parameters as used, accounted only for changes in the wrinkling of the flame shape. The authors claim that they will be able to capture the bulk motion of the flame observed in test rigs merely by changing some parameters, but this is still work in progress.

The objective of the work presented in this paper is to characterize unstable combustion in a lean premixed dump combustor over a broad range of operating conditions and to study the relative contributions of equivalence ratio fluctuations and flame–vortex interactions to the observed heat-release fluctuations. In the first phase of the study, a variety of parameters were varied, and their effect on stability was investigated. The parameters were chosen based on the knowledge that they affected flame stabilization. Optical visualization techniques were then used, including acetone laser-induced fluorescence to characterize the combustor inlet fuel distribution and CH chemiluminescence to characterize the heat-release structure and its relationship to unstable combustion. Based on the chemiluminescence images, a simple analysis was carried out to identify the contributions to the heat-release fluctuation from different sources.

Experimental Setup

A coaxial dump combustor with a rearward-facing step was used (Fig. 1). The combustor has a diameter of 108 mm and a length of 850 mm and is made of fused silica to provide optical access. The length was chosen after a series of experiments conducted to determine the length most susceptible to unstable combustion. That the aspect ratio has an effect on combustion stability has been observed previously by Sivasegaram and Whitelaw.[16] The mixing section has a diameter of 36 mm and a length of 870 mm. The flame is stabilized using a bluff centerbody (19 mm diam) located at the exit of the mixing section. This distinguishes it from the studies that have been conducted on ramjet combustors or models of ramjet combustors.[7–11] In those cases the flame is stabilized on the step itself, resulting in a flame whose structure is that of a cone with its base on the dump plane. This is markedly different from a flame stabilized on a bluff centerbody, which is also conical but has its base downstream. Considering the importance of flame–flowfield interactions on combustion stability, such a difference in the flame structure is likely to result in a marked change in the stability characteristics.

The fuel used is natural gas (96% methane) and is introduced into the mixing section at two locations in various proportions. The first location is well upstream (~60 mixing section diameters) of the dump plane resulting in a uniform fuel–air mixture at the combustor inlet. The other location is 25.4 mm upstream of the dump plane in the form of 16 holes (of diameter 0.41 mm each), equally spaced

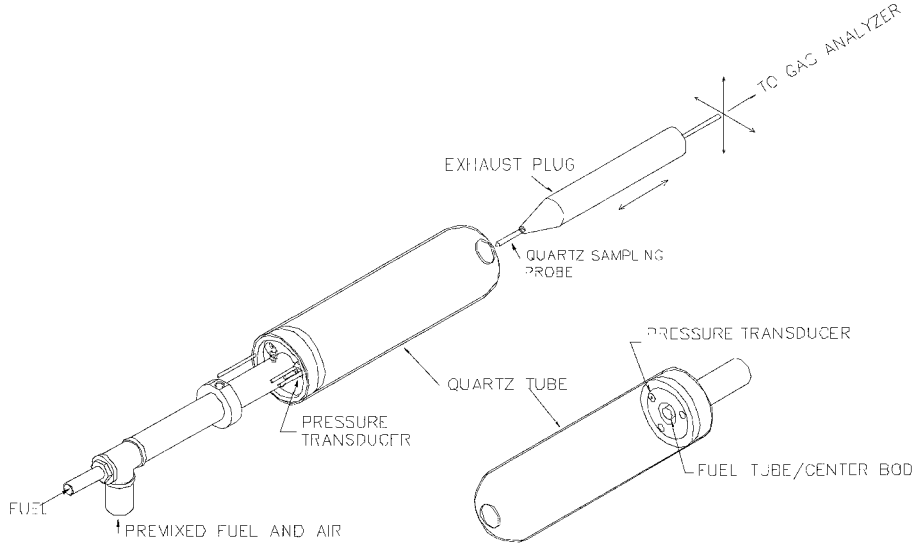

Fig. 1 Schematic of the dump combustor.

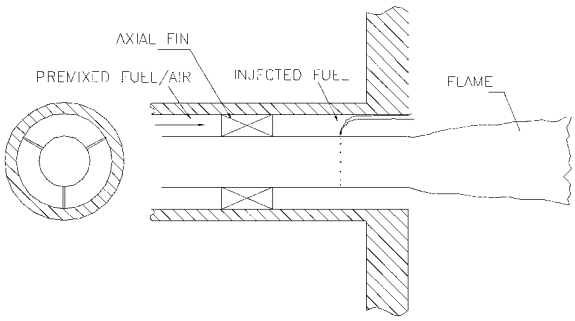

Fig. 2 Closeup of mixer section.

around the circumference of the centerbody, resulting in a nonuniform fuel distribution concentrated in the outer shear layer of the mixing tube. A 20-kW electric heater is used to heat the airflow, and a thermocouple 10 mm upstream of the dump plane is used in conjunction with a temperature controller to regulate the inlet temperature of the mixture. The centerbody is centered in the mixing section using vanes that also serve as axial swirlers. The flat-vaned axial swirler has an estimated swirl number of 0.46 for a vane angle of 30 deg and an estimated swirl number of 1.37 for a vane angle of 60 deg (Ref. 23). A closeup of the mixing section detailing the centerbody, swirl vanes, and injection holes near the dump plane is shown in Fig. 2. High-frequency pressure transducers, flush mounted at the dump plane and in the mixing section, are used to measure the pressure oscillations. A water-cooled gas-sampling probe, supported by a conical exhaust plug, is used to extract gas samples from the exhaust. NO_x, CO, and O_2 concentrations in the exhaust gases are measured using continuous gas analyzers. The exhaust plug can be used to increase the pressure inside the combustor by partially blocking the exit of the combustor. A pulsed Nd-YAG laser and an intensified charge-coupled device (CCD) camera are used to make laser-induced fluorescence (LIF) measurements to characterize the fuel distribution at the exit of the mixing section. The intensified CCD (ICCD) camera is also used to record CH chemiluminescence images of the flame zone that define the heat-release structure in the combustor.

Procedure

Stability Characteristics

As a first step toward understanding the instability mechanism, the stability characteristics of the combustor were determined. The aim of this part of the study was twofold. One goal was to identify unstable operating conditions for further study; another was to determine the effects of specific parameters on combustion stability, where any mechanistic explanation of unstable combustion must be consistent with these observations. To this end, the peak-to-peak pressure amplitude of the dump-plane pressure transducer was plotted against equivalence ratio in a series of stability maps. The stability maps were always measured by increasing the equivalence ratio, inasmuch as preliminary tests indicated that the stability limits of the combustor varied depending on the direction in which the equivalence ratio was changed due to hysteresis effects. At all operating conditions, a Fourier transform was also carried out on the signal from the dump-plane pressure transducer to extract the dominant frequencies of the instability.

The parameters varied were inlet swirl, centerbody recess, and inlet fuel distribution. For each set of parameters, at a particular velocity, the equivalence ratio was varied from lean blowout to stoichiometric, and then the velocity was varied from 2 to 6 m/s ($Re_{\text{comb}} \sim 10^4$, $Re_{\text{mixer}} \sim 10^5$). The inlet swirl was varied by altering the vane angles on the bluff centerbody. Three swirl cases were studied, that is, 0, 30, and 60 deg. The centerbody recess was effected by moving the centerbody along the mixing section. The four cases studied were $0D$, $1/4D$, $1/2D$, and $1D$ recess, where D is the diameter of the centerbody. The inlet fuel distribution was controlled by changing the proportion of premixed fuel and injected fuel. The proportion was varied from 100% premixed fuel, referred to as the 100% premixed condition, to 50% premixed and 50% injected fuel, referred to as the 50% premixed condition. Because of the nature of the fuel distribution (discussed later), at higher proportions of injected fuel, the flame tends to be detached throughout the flammable range. This restricts the range of comparable operating conditions to those with less than 50% injected fuel.

Acetone LIF

To determine the fuel distribution at the dump plane, acetone planar LIF was used. The ability of acetone to act as a tracer for gaseous fuels was demonstrated by Lozano et al.[24] Based on the results of tests carried out to identify the temperature at which the fluorescence intensity (using 266-nm excitation) was the strongest, the inlet temperature of the air–fuel mixture was set at 200°C. The fourth harmonic of a pulsed Nd-YAG laser (~10 mJ at 266 nm) was used to excite the acetone, and the fluorescence images were captured using an ICCD camera (Princeton Instruments 576a) and a high-pass filter with a cutoff frequency of 335 nm (WG-335). Using a combination of spherical and cylindrical lenses, the laser beam was formed into a collimated sheet with a thickness of less than 1 mm (over the field of view) and a width of ~2.5 cm.

The fuel distribution was measured for 100, 75, 50, 25, and 0% premixed conditions. The acetone concentration used in these tests was nominally 2%. At each condition, fluorescence images were acquired at two inlet velocities, 3 and 5 m/s, and at each velocity, images were captured at overall equivalence ratios of 0.6 and 0.9. At a particular overall equivalence ratio and inlet velocity, the 100% premixed image was used to normalize the partially premixed images and, thus, convert the measured fluorescence intensities to equivalence ratios. Because these measurements were made without combustion, natural gas was replaced with nitrogen for safety reasons. Care was taken to match the volumetric flow rates of nitrogen and natural gas for the premixed fuel and their momentum fluxes for the injected fuel. The final image was an average of 100 individual images thus removing any temporal effects. The background image, which was also an average of 100 images, was first subtracted from the averaged image. The background subtracted image was then normalized with the corresponding background subtracted premixed image. To calculate the inlet fuel profile, intensities of six adjacent pixels at the same radial location, about 1.8 mm downstream of the dump plane, were averaged and plotted against their radial location.

CH Chemiluminescence

Phase-resolved CH chemiluminescence imaging was used to characterize the spatial and temporal evolution of the heat-release structure in the combustor at selected unstable operating conditions. Chemiluminescence from a variety of flame radicals, including CH, CO_2^*, and OH, has been used as an indicator of both local[25,26] and global[27] heat release in lean premixed hydrocarbon flames. Recent studies,[28] however, have shown that the HCO radical is a more accurate indicator of local heat release in highly stretched flames. Although it is clear that flame stretch effects will be important in terms of certain aspects of lean premixed gas turbine combustion, such as lean blowout and CO emissions due to flame quenching, it is also reasonable to assume that the bulk of the heat release will occur under conditions where flame stretch is not an important factor, particularly with a fuel that is predominately methane.[29–31] Another issue with respect to using chemiluminescence intensity as an indicator of the heat release is the functional relationship between these two quantities. Bandaru et al.[27] have shown, for example, that CH chemiluminescence intensity varies nonlinearly with equivalence ratio from lean blowout to stoichiometric conditions. Their results also show, however, that over a small range of fuel–lean equivalence ratios that this behavior can be reasonably approximated as linear. In the work presented in this paper, such a linear relationship is assumed.

The ICCD camera with a bandpass filter centered at 430 nm (±5 nm bandwidth) was used to capture the CH chemiluminescence images. The field of view was 152 × 114 mm. To trace the development of the heat-release structure through one period of the

instability, the measurement was phase synchronized with the pressure signal from the combustor. At each phase angle 32 individual images were taken and were averaged to represent the heat-release structure at that phase angle. Averaged images were acquired at 12 different phase angles over the time period of each pressure oscillation. The phase-averaged value of the fluctuating pressure at the dump plane was also recorded at each phase angle and was then used for further analysis of the heat-release data.

Deconvolution

The CH chemiluminescence images captured using the procedure just described were line-of-sight images. This resulted in a distorted picture of the actual heat-release structure. A three-point Abel deconvolution scheme[32] was used to extract two-dimensional data from the line-of-sight images. The inversion procedure assumes axisymmetry, whereas the flame images were slightly asymmetric. For the purpose of deconvolution, however, intensities at the same axial coordinate and at equal radii were averaged to artificially make the images axisymmetric. Also implicit in this procedure is the assumption that the intensity at each pixel has its source along a line of sight that is perpendicular to the surface of the pixel, which, again, is not completely true. Off-axis points also contribute to the intensity at each pixel. To minimize this error, the camera has to be as far away from the source as possible. As is typical of the Abel deconvolution procedure, some noise was observed along the centerline of the reconstructed image. This was in the form of a very thin band of approximately five pixels (1.4 mm) with inordinately high-intensity values. The image was smoothed around the centerline, and the noise was artificially removed. The deconvoluted images were then used for all further analyses.

Analyses of CH Images

Besides visual inspection, several different analyses were performed on the CH images. In particular, flame area and total chemiluminescence intensity were calculated at each phase angle, whereas the Rayleigh index was evaluated as a function of position in the flame.

The flame area was calculated from the deconvoluted two-dimensional chemiluminescence images. Based on estimates of the turbulent Damkohler number and turbulent Reynolds number, one can assume that under the conditions of these experiments that combustion was in the wrinkled laminar flame regime.[33] Therefore, the two-dimensional chemiluminescence images effectively represent a two-dimensional turbulent flame brush. To calculate the flame area, first the maximum intensity throughout the flame brush is identified. Then the boundary of the flame brush is fixed by defining any pixel that has an intensity greater than 5% of the maximum intensity as part of the flame. Once the perimeter of the flame brush has been defined, pixels of maximum intensity in the flame are identified on lines locally perpendicular to the flame brush. The line joining these pixels represents the average two-dimensional flame sheet. The three-dimensional surface area of the flame sheet is defined by the surface of revolution of the average two-dimensional flame sheet around the centerline of the combustor. It is important to recognize, however, that this flame area is the average, or what might be called the laminar, flame area. Therefore, it is not the actual flame area because it does not include the flame area associated with the turbulent wrinkling of the flame surface. This point will be addressed again later.

Total chemiluminescence intensity is calculated by summing the intensities of all of the pixels that are part of the flame brush, weighted by the radial location of each pixel to account for the annular volume represented by each pixel.

The local Rayleigh index $R(x, r)$ is given by

$$R(x, r) = \frac{1}{T} \int 2\pi r p'(t) q'(x, r, t)\, \mathrm{d}t \qquad (1)$$

where p' is the fluctuating pressure and q' is the fluctuating heat release.[20] Implicit is the assumption that the pressure measured at the dump plane is the pressure over the entire flame. This is a reasonable assumption because the flame length ($\leq$5 cm) is much shorter than the wavelength of the pressure wave ($\sim$170 cm). Hence, at any given time, the pressure is effectively uniform over the flame surface. The time integral in the Rayleigh index calculation is approximated by a sum over the 12 images. The local Rayleigh index represents the correlation between the local pressure oscillation and the local heat-release oscillation. As proposed by Rayleigh,[6] regions that act as drivers of the instability have a high correlation between pressure and heat release, and hence a positive Rayleigh index, whereas regions that damp the instability have a negative Rayleigh index.

Results and Discussion

The first results to be presented are from tests carried out to determine the stability characteristics of the combustor at the baseline condition, that is no swirl, no centerbody recess, 400°C inlet temperature, and 100% premixed. These results are presented in the form of stability maps that are plots of the amplitude of the peak-to-peak pressure fluctuations in the combustor vs the overall equivalence ratio.

Figure 3 shows the stability maps for different inlet velocities at the baseline condition. The leftmost point on each curve is the lean blowout limit for that velocity. Combustion is defined to be unstable if there is a marked increase in the amplitude of the pressure fluctuations for a relatively small increase in equivalence ratio and if the frequency spectrum of the pressure fluctuations reveals a dominant frequency or frequencies. For example, in the 6-m/s case, as the equivalence ratio is increased from the lean blowout limit, combustion first becomes unstable around an equivalence ratio of 0.55, then it restabilizes at about an equivalence ratio of 0.8, and then it becomes unstable again as the equivalence ratio approaches stoichiometry. This trend, including the values of the equivalence ratio at which combustion changes from stable to unstable and vice versa, is repeatable from day to day. If the 6-m/s result is compared to the results at lower velocities it is apparent that the tendency for combustion to become unstable increases as the inlet velocity increases. Similar results have been obtained by Katsuki and Whitelaw,[34] who noted that the stable range of combustion in a bluff-body stabilized flame decreased with increasing Reynolds number.

The frequency spectra of the pressure signal for all of the unstable conditions at the baseline operating condition exhibit a dominant frequency at about 490 Hz ($\pm$50 Hz), and as the strength of the instability increases, higher harmonics also begin to appear. If an average temperature in the combustor is assumed, the frequencies of longitudinal-, transverse-, and bulk-mode instabilities in this combustor can be calculated. For a temperature of 1700 K, one calculates a longitudinal half-wave frequency of 470 Hz, a fundamental transverse-mode frequency of 4000 Hz, and a bulk-mode frequency of 150 Hz. Comparing these to the measured frequency of 490 Hz indicates that this is a longitudinal-mode instability. As equivalence

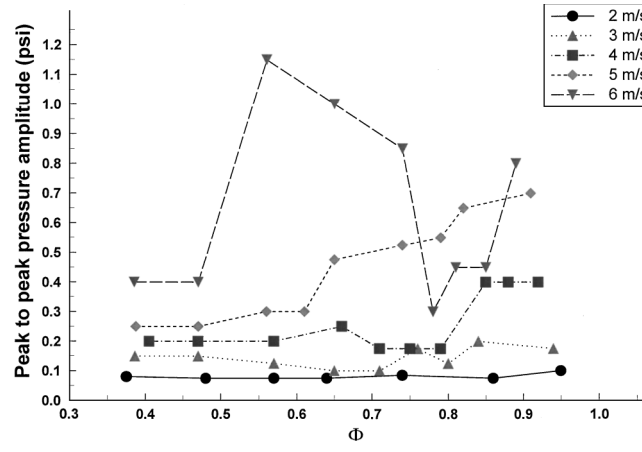

Fig. 3 Stability maps for different inlet velocities at the baseline condition.

ratio increases, the frequency of the instability is found to increase. This is consistent with the wavelength remaining constant (fixed by the length of the combustor) while the sound speed increases due to the rise in flame temperature.

Phase-resolved CH chemiluminescence images for the unstable baseline operating condition at 6 m/s and $\phi = 0.6$ are presented next. Figure 4a shows the line-of-sight chemiluminescence images, and Fig. 4b shows the corresponding deconvoluted two-dimensional images. The locations of the mixer and centerbody are shown for reference. Both sets of images show evidence of periodic shedding of vortices from the dump plane and their interaction with the flame; however, this is more clearly seen in the deconvoluted images. The deconvoluted images also show that there is no heat release on the centerline of the combustor, as one would expect. It can be seen from the images, which are taken over one period of pressure oscillation, that one vortex is shed every period. This indicates a vortex shedding frequency equal to the instability frequency and well removed from the natural shedding frequency, which is of the order of 2000 Hz (Ref. 11). The difference between the natural shedding frequency and the forced shedding frequency reveals a strong interaction between the fluid dynamics at the step, that is, vortex shedding, and the acoustics of the combustor. Similar results have been obtained for all of the unstable baseline conditions at which images were acquired, suggesting that flame–vortex interaction plays an important, if not critical, role in the instabilities observed at these conditions.

The stability maps in Fig. 3 indicate that a small increase in equivalence ratio results in a stable flame becoming unstable. A possible explanation for this behavior, based on flame–vortex interaction, is shown in Fig. 5. Two possible flame–vortex configurations are shown. In the first, which is at the lower equivalence ratio, the flame and vortex do not interact. In the second, which is at a slightly higher equivalence ratio, the flame has widened due to its increased flame speed and, as a result, does interact with the vortex.

Figures 6–8 show the results of the analyses carried out on the two-dimensional deconvoluted CH images presented in Fig. 4b. The Rayleigh index distribution (Fig. 6) indicates that at this operating condition the instability is most strongly driven in the outer shear layer, about 100 mm downstream of the dump plane. This

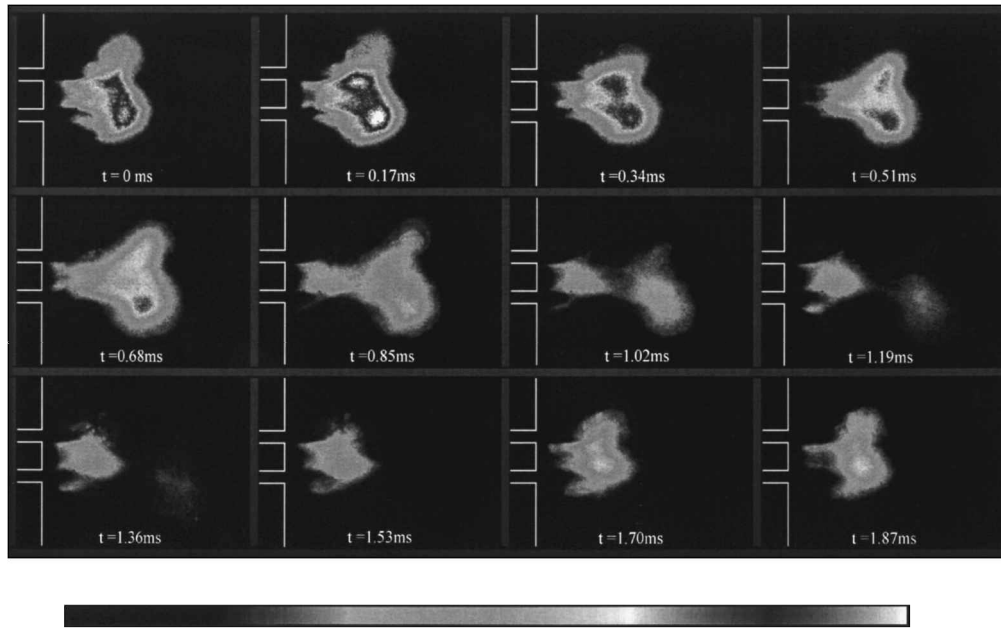

Fig. 4a Line-of-sight chemiluminescence images at 6 m/s, Φ = 0.6, 0-deg swirl, 0*D* recess, 100% premixed, inlet temperature of 400°C, and *T* = 2.05 ms.

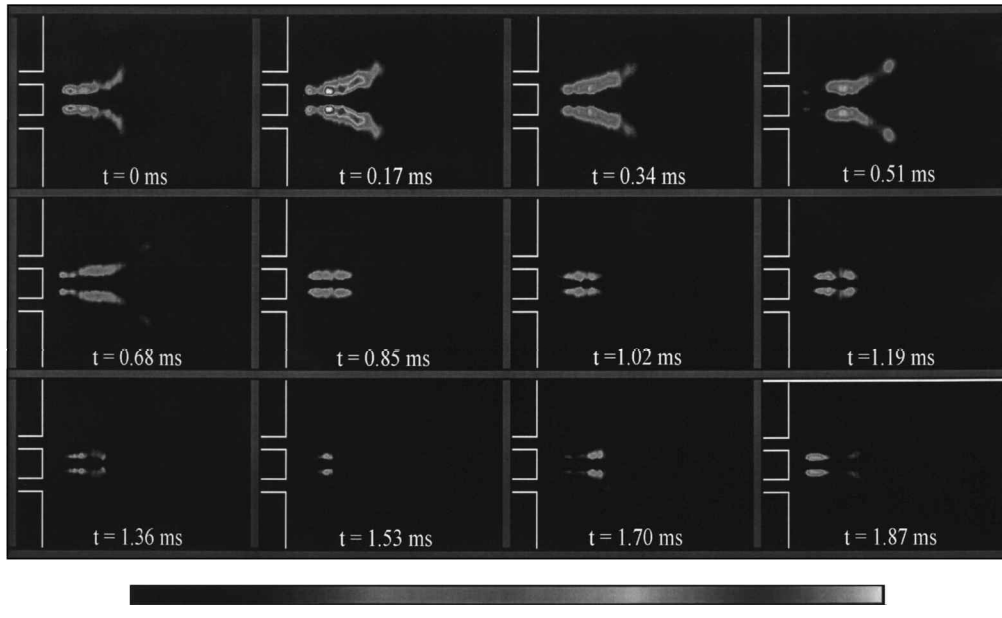

Fig. 4b Deconvoluted CH chemiluminescence images at 6 m/s, Φ = 0.6, 0-deg swirl, 0*D* recess, 100% premixed, inlet temperature of 400°C, and *T* = 2.05 ms.

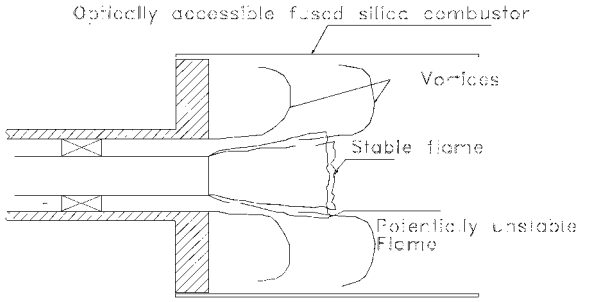

Fig. 5 Schematic of flame–vortex interaction.

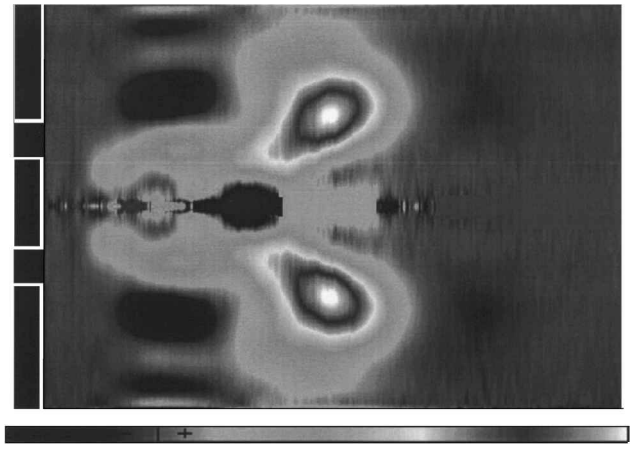

Fig. 6 Rayleigh index distribution for the conditions in Fig. 4b.

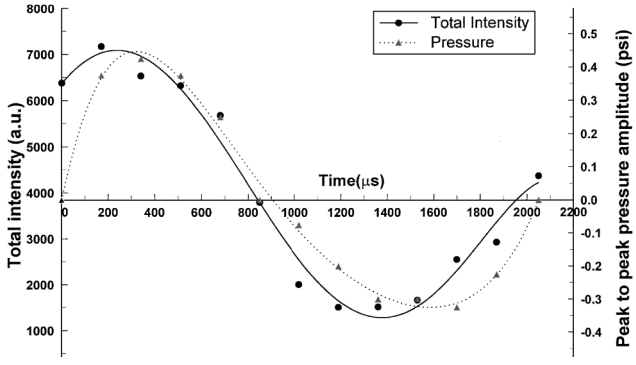

Fig. 7 Variation of total intensity and pressure over one period of oscillation for the conditions in Fig. 4b.

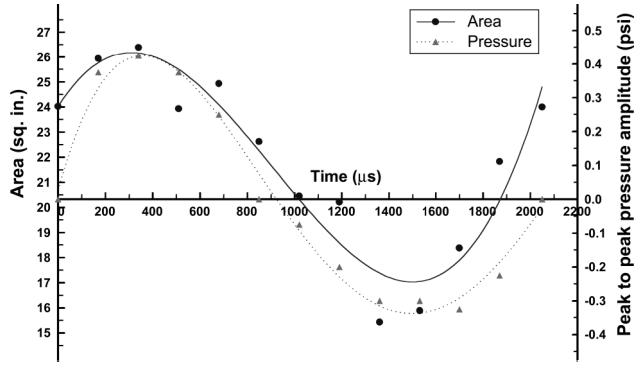

Fig. 8 Variation of flame area and pressure over one period of oscillation for the conditions in Fig. 4b.

is consistent with the preceding observations regarding the role of flame–vortex interaction in the observed instabilities. It is also clear that the overall Rayleigh index, which is the spatial integral of the local Rayleigh index over the entire flame zone, is positive. Rayleigh index distributions for other inlet velocities and overall equivalence ratios, at the baseline operating condition, show that the driving regions are approximately at the same radial location; however, they move closer to the dump plane as the inlet velocity decreases. Flame–vortex interaction suggests a possible explanation for this behavior. Note that the frequency of the instability remains approximately the same, irrespective of velocity, and that the time available for the vortex to convect downstream is approximately half a time period; therefore, at lower velocities, the vortex convects a smaller distance in the time available. This implies that the flame fluctuates over a shorter distance from the dump plane, thus moving the driving zone closer to the dump plane.

Figure 7 shows the variation of total chemiluminescence intensity with time over one period of pressure oscillation for the conditions in Fig. 4b. Because the chemiluminescence intensity is proportional to the flame's heat release, this result is in agreement with Rayleigh's criterion that states that, for combustion to be unstable, the fluctuating heat release has to be in phase with the fluctuating pressure. The result in Fig. 7 shows that the heat-release fluctuation leads the pressure fluctuation by approximately 36 deg. This is contrary to the notion that, in combustion systems with small acoustic losses, the heat-release fluctuation and the pressure fluctuation have to be in quadrature.[10] However, phase differences significantly less than 90 deg have also been observed by a number of authors, including Langhorne,[35] Keller and Saito,[36] and Fernandes and Heitor.[37]

The variation in flame area for the results shown in Fig. 4b is shown in Fig. 8. This result shows that the flame area fluctuations are also very nearly in phase with the pressure oscillation, suggesting that flame area fluctuations play a role in the observed heat-release fluctuations. A similar observation based on flame length fluctuations was made by Reuter et al.[38] It is not clear, however, from their results whether the heat-release fluctuation can be attributed entirely to flame area fluctuations because other factors, for example, equivalence ratio fluctuations, were not addressed.

To identify the relative contributions of flame area and equivalence ratio fluctuations to the heat-release fluctuation, the following simple analysis was carried out. By the assumption that the flame is in the wrinkled laminar flame regime, the elemental mass flow rate of unburned fuel and air flowing into the flame can be given by

$$\mathrm{d}\dot{m}_t = \rho_u S_l \,\mathrm{d}A \tag{2}$$

where ρ_u is the density of the unburned gas, S_l is the laminar flame speed, and $\mathrm{d}A$ is the elemental flame area. In general ρ_u and S_l may vary along the flame front. By the utilization of the relationship between the total air and fuel flow rate $\dot{m}_t$, the fuel flow rate $\dot{m}_f$, and the equivalence ratio ϕ, this equation can be written in terms of the elemental fuel flow rate, which is the fuel flow rate through $\mathrm{d}A$, as follows:

$$\mathrm{d}\dot{m}_f = \rho_u S_l \frac{0.05\phi}{1 + 0.05\phi}\,\mathrm{d}A \tag{3}$$

where 0.05 is the stoichiometric mass-based fuel–air ratio for natural gas and air. The elemental heat-release rate $\mathrm{d}\dot{Q}$ is then given by

$$\mathrm{d}\dot{Q} = \rho_u S_l \frac{0.05\phi}{1 + 0.05\phi}\mathrm{HV}\,\mathrm{d}A \tag{4}$$

where the heating value (HV) of the fuel is at the temperature of the unburned gas T_u. If we assume that the reactants behave as an ideal gas, this can be written as

$$\mathrm{d}\dot{Q} = \frac{P}{R_u T_u}\frac{1 + 0.05\phi}{0.57 + 0.05\phi}\mathrm{MW}_f\,\mathrm{HV}\,S_l\frac{0.05\phi}{1 + 0.05\phi}\mathrm{d}A \tag{5}$$

where MW_f is the molecular weight of natural gas and 0.57 is the ratio of the molecular weight of natural gas to that of air. If it is

assumed that the laminar flame speed is proportional to the equivalence ratio, that is, $S_l = C_1 \cdot \phi$, which is a reasonable assumption under fuel lean conditions,[33] then Eq. (5) reduces to

$$\mathrm{d}\dot{Q} = \frac{\mathrm{HV}\ \mathrm{MW}_f}{R_u T_u} C_1 P \frac{0.05\phi^2}{0.57 + 0.05\phi} \mathrm{d}A \tag{6}$$

In this case, C_1 is a constant because the inlet temperature is fixed and because pressure has negligible effect on flame speed at the equivalence ratios and pressures under study.[34] Stretch effects, which can also play an important role in flame speed determination, may not be negligible, but for the purposes of this analysis, they are assumed to be. This may not be a bad assumption because the fuel is composed predominantly of methane (~96%), which has a Lewis number close to unity.[35–37]

Although pressure and equivalence ratio are fluctuating with time, it is reasonable to assume that at a given instant of time that the pressure and the equivalence ratio are uniform over the entire flame. For this to be true, the length of the flame zone (≤5 cm for the flame shown in Fig. 4b) must be much smaller than the wavelengths of both the pressure and equivalence ratio oscillations in the unburned gas, which would be the acoustic and the convective wavelengths, respectively. For the flame shown in Fig. 4b, the acoustic wavelength is approximately 170 cm, and the convective wavelength is approximately 20 cm. Therefore, it is certainly reasonable to assume that the pressure is uniform over the flame zone at any instant of time, but this is only marginally true for the equivalence ratio. In addition, T_u can be assumed to be a constant, independent of both space and time. Hence, Eq. (6) can be integrated over the area of the flame yielding

$$\dot{Q}(t) = C_2 A(t) P(t) \frac{0.05\phi^2(t)}{0.57 + 0.05\phi(t)} \tag{7}$$

$$\dot{Q}(t) = C_2 A(t) P(t) f(t) \tag{8}$$

where $C_2 = \mathrm{HV} \cdot \mathrm{MW}_f \cdot C_1 / R_u T_u$, $f(t) = 0.05\phi^2(t)/[0.57 + 0.05\phi(t)]$ represents the combined effects of equivalence ratio on heat release, and $P(t)$ is the effect of fluctuating pressure, that is, density, on heat release. Equation (8) is very similar in form to the equation that Peracchio and Proscia[21] used in their study. Whereas they also used a linear relationship between $\dot{Q}$, A, and P, the difference was that they used time-lag concepts to calculate $f(t)$ at the dump plane.

Because $P(t)$ is measured, whereas $\dot{Q}(t)$ and $A(t)$ are determined from the CH images, Eq. (8) can be used to calculate $f(t)$. Note that the flame area needed in Eq. (8), however, is actually the turbulent flame area, whereas the flame area that is calculated from the CH chemiluminescence images is the average flame area, which is representative of what would be called the laminar flame area. Therefore, to use the measured flame area in Eq. (8), it is necessary to assume that the turbulent to laminar flame area ratio is a constant during the instability, and then this constant becomes part of C_2. In general, the ratio of the turbulent to laminar flame area is a function of the turbulence intensity and the turbulence length scales. Therefore, this assumption implies that the turbulence properties of the flow do not change during the instability.

Equation (8) can now be used to determine the relative contributions of flame area, pressure, and equivalence ratio fluctuations to the observed total heat-release fluctuations. To do this, $C_2 f(t)$ is first calculated at all of the data points using the measured values of $\dot{Q}$, P, and A. Equation (8) is then written in differential form as

$$\mathrm{d}\dot{Q} = C_2 \phi_h A\, \mathrm{d}P + C_2 \phi_h P\, \mathrm{d}A + C_2 A P\, \mathrm{d}f(\phi, t) \tag{9}$$

The three terms on the right-hand side of Eq. (9) represent the relative contributions to the differential change in the heat release due to a differential change in pressure, a differential change in flame area, and a differential change in equivalence ratio, respectively. (Note that although the particular operating condition being considered is 100% premixed, temporal equivalence ratio oscillations still can occur because the fuel flow is choked and, therefore, constant, while the air flow rate is fluctuating.[39]) Beginning at the phase angle that has the mean heat release, that is, the heat-release fluctuation is zero, each term in Eq. (9) is calculated for each time step, and then the cumulative sum of each term is plotted with time in Fig. 9. It can be seen that the contributions due to flame area fluctuations and equivalence ratio fluctuations are of the same order, whereas the contribution from pressure, that is, density, fluctuations is negligible. This indicates that the heat-release fluctuation, in this case, is associated with both flame area and equivalence ratio fluctuations.

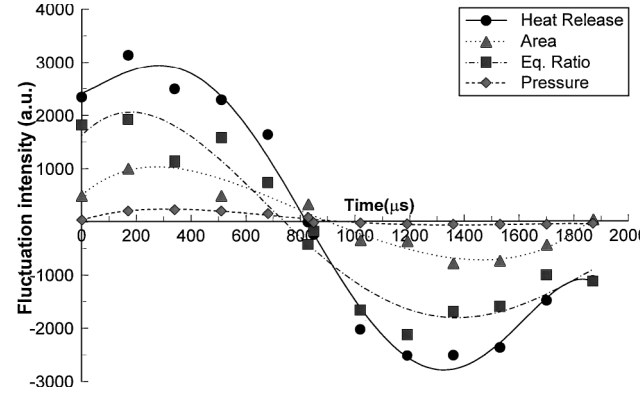

Fig. 9 Contributions to heat release fluctuations from different sources.

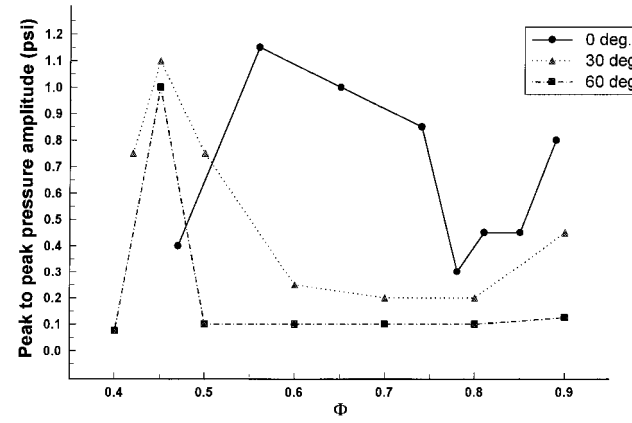

Fig. 10 Stability map showing the effect of swirl.

The results presented and discussed so far have been for the baseline conditions, that is, no swirl, no centerbody recess, and 100% premixed fuel and air. In the following, the effects of swirl, centerbody recess, and the combustor inlet fuel distribution on the stability characteristics of this combustor are presented and discussed.

The effect of swirl on the stability characteristics of the combustor is shown in Fig. 10 for the 6-m/s, 400°C, 100% premixed operating condition. As shown in Fig. 10, the effect of swirl is to stabilize the combustion process at higher equivalence ratios and to introduce a new regime of unstable combustion at equivalence ratios close to lean blowout. Stabilization at higher equivalence ratios with swirl is possibly due to the disruption of the normal vortex shedding patterns. Ahmed and Nejad[40] noted that the corner recirculation zone significantly reduces in size with swirl. The same effect was also noted by Sivasegaram and Whitelaw,[41] who observed that the length of the corner recirculation zone was reduced by 33% when the inlet swirl number was changed from 0 to 0.46. This, possibly, decreases the chance of flame–vortex interaction resulting in more stable combustion. The new instability regime, that is, near lean blowout, is most likely due to rapid detaching and reattaching of the flame from the bluff centerbody, as opposed to flame–vortex interaction, and can be associated with the central toroidal recirculation zone that

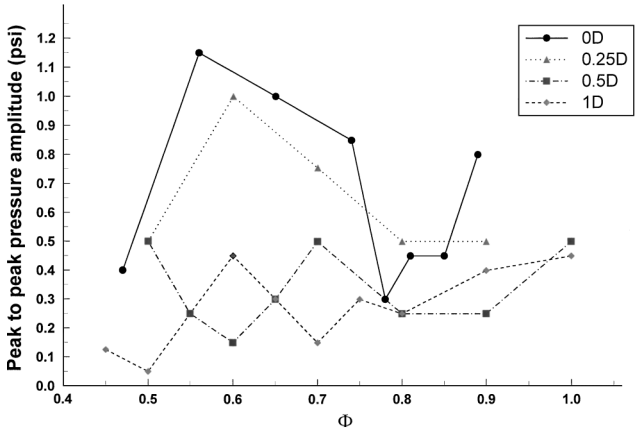

Fig. 11 Stability maps showing the effect of centerbody recess.

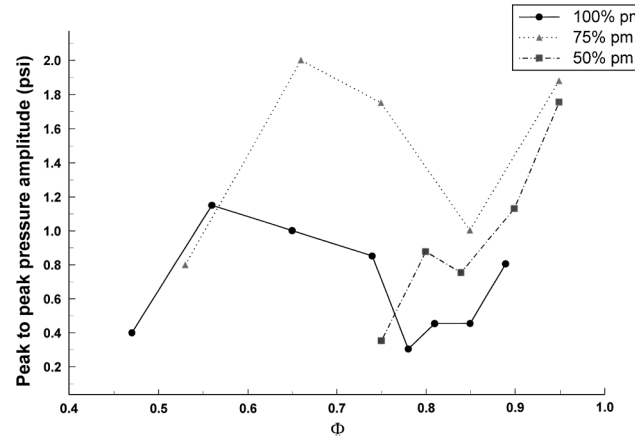

Fig. 12 Stability effects showing the effect of partial premixing.

forms in front of the centerbody with strong inlet swirl.[40] Note, however, that there is no change in the frequency of the instability, indicating that there is no change in the mode of the instability either. This is unlike the result of Logan et al.,[5] who observed a bulk-mode instability near lean blowout as compared to a longitudinal-mode instability at higher equivalence ratios.

The effect of centerbody recess on combustion stability is presented in Fig. 11 for the 6-m/s, 400°C, no-swirl, 100% premixed operating condition. The baseline case with no centerbody recess is the most susceptible to unstable combustion. As the centerbody is recessed, combustion becomes stable over a wider range of equivalence ratios, until at a centerbody recess of $1/2D$, no instabilities are observed. Assuming that flame–vortex interaction is responsible for the instabilities in the no-swirl case with no centerbody recess, it seems reasonable to speculate that recessing the centerbody alters this interaction and, therefore, stabilizes the combustion. There are two possible explanations why flame–vortex interaction becomes less important as the centerbody is recessed. One is simply that a significant portion of the flame, and hence the heat release, occurs inside the mixing tube and, therefore, upstream of the dump plane where the vortex is formed. The other is that because the flame is partially confined by the mixing tube, it is narrower than in the case with no centerbody recess. Therefore, the flame interacts less with the vortex that is shed at the dump plane.

That flame–vortex interaction seems to play a role in all of the instabilities that were observed without swirl suggests that it may also offer an explanation for the effect of increasing inlet velocity on the stability characteristics at the baseline condition. The effectiveness of the interaction between the flame and the vortex depends on the coherence or strength of the vortex. Because increasing Reynolds number increases the coherence of the vortex, it is reasonable to speculate that this in turn increases the effectiveness of the flame–vortex interaction.

The effect of inlet fuel distribution on combustion stability is shown in Fig. 12 for the 6-m/s, 400°C, no-swirl, no centerbody recess operating condition. However, before discussing these results it is important to comment briefly on the relationship between the inlet fuel distribution and incomplete fuel–air mixing. Although incomplete fuel–air mixing in lean premixed combustors is undesirable because of its effect on NO_x emissions, that is, incomplete mixing increases NO_x emissions, its effect on stability is not clear.[13,42] This is because whenever there is incomplete fuel–air mixing there is almost always a gradient in the mean fuel distribution that itself can have a significant effect on stability. This is illustrated in the following discussion of the results shown in Fig. 12. The three cases shown in Fig. 12 are the so-called 100% premixed, 75% premixed, and 50% premixed conditions. The first observation is that the lean limit shifts to higher equivalence ratios as the percentage of premixed fuel decreases, where the lean limit is defined as the lowest equivalence ratio for which the flame is anchored on the centerbody. The reason for this becomes apparent after considering the inlet fuel distribution in the partially premixed cases. Figure 13 shows the inlet

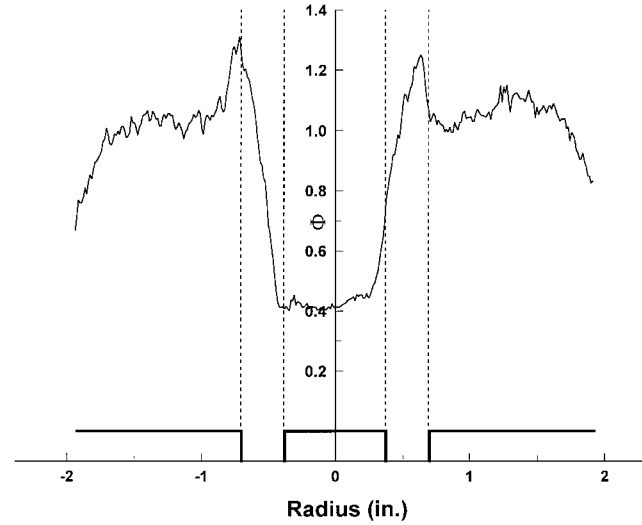

Fig. 13 Inlet fuel distribution.

fuel distribution for an inlet velocity of 5 m/s, an overall equivalence ratio of 0.9, no-swirl, no centerbody recess, and 50% premixed conditions. The end of the centerbody and the mixer exit are shown for reference. This result is typical of all of the partially premixed conditions in that the equivalence ratio increases from a minimum along the centerbody to a maximum along the wall of the mixing tube. For example, in the 50% premixed case with an overall equivalence ratio of 0.9, the equivalence ratio varies from a minimum of 0.6 at the centerbody to a maximum of 1.2 at the mixing tube. Therefore, the overall equivalence ratio required to have an equivalence ratio at the centerbody that is sufficient to anchor the flame increases as the percentage of premixed fuel decreases.

In terms of the effect of the inlet fuel distribution on the stability characteristics of this combustor, the results in Fig. 12 indicate that as the percentage of premixed fuel decreases there is a significant increase in the strength of the instability, both in the midrange of equivalence ratios and at near stoichiometric conditions. The tendency for combustion to restabilize at equivalence ratios near 0.8 is still evident in the partially premixed cases, but it is not as pronounced as it is in the 100% premixed case.

Again, because there is no swirl in these cases, it is interesting to attempt to explain this behavior in terms of flame–vortex interaction. As the fuel distribution measurements show, in the partially premixed cases, the fuel concentration is greater along the outer wall of the mixing tube than along the centerbody. This suggests that the reaction zone, that is, the flame, is likely to move radially outward as the percentage of premixed fuel decreases and as a result be more susceptible to flame–vortex interactions. Rayleigh index plots for instabilities under nonpremixed conditions support this conjecture in

that they show that as the proportion of the injected fuel is increased, the location of the maximum Rayleigh index moves outward from a radial location 25 mm from the centerline for the premixed condition to a radial location 30 mm from the centerline. Again, this is evidence of the importance of considering the effect of the fuel distribution when considering the effect of incomplete mixing on the stability characteristics of lean premixed combustors.

Conclusions

A study of unstable combustion in lean premixed combustors was conducted in a bluff-body-stabilized dump combustor. A parametric study was carried out, and equivalence ratio, inlet velocity, inlet fuel distribution, centerbody recess, and swirl were all found to affect combustion stability. For the case of combustion without swirl, increasing equivalence ratio and increasing inlet velocity were found to increase the susceptibility to unstable combustion whereas increasing the centerbody recess was found to stabilize combustion. Regarding the effect of the inlet fuel distribution, it was noted that it is important to distinguish between the effect of incomplete fuel–air mixing and the effect of the inlet fuel distribution on the stability characteristics of a lean premixed combustor. CH chemiluminescence images were captured at a variety of unstable operating conditions, and a three-point Abel deconvolution procedure was employed to extract two-dimensional data from the line-of-sight images. Rayleigh index distributions were calculated from these two-dimensional images and were used to identify driving regions of the instability. These results indicated that vortex shedding plays an important role during unstable combustion when there is no swirl. In fact, most of the instability characteristics observed without swirl could be explained in terms of flame–vortex interactions. The variation of pressure, flame area, and total heat release was also compared. A simple analysis revealed that without swirl the heat-release oscillation was associated with both flame area fluctuations and equivalence ratio fluctuations. A fundamental difference appears to exist between the instability mechanism with and without swirl. Whereas swirl stabilizes combustion at higher equivalence ratios, it seems to introduce instability at equivalence ratios near the lean blowout limit. In summary, this study shows the importance of characterizing flame–flowfield interactions in understanding unstable combustion.

Acknowledgments

Support for this research has been provided by General Electric Aircraft Engines, United Technologies Research Center, and the Air Force Office of Scientific Research. In addition, B. J. Lee was partially supported by the Korean Science and Engineering Foundation and L. H. Preston was supported by a Department of Education Graduate Assistance in Areas of National Need (GAANN) Fellowship.

References

[1]Feitelberg, A. S., and Lacey, M. A., "GE Rich-Quench-Lean Gas Turbine Combustor," American Society of Mechanical Engineers, Paper 97-GT-127, June 1997.

[2]Hayashi, S., "Compatibility Between Low NOx Emissions and High Combustion Efficiency by Lean Direct Injection Combustion," American Society of Mechanical Engineers, Paper 95-GT-276, June 1995.

[3]Correa, S. M., "Review of NOx Formation Under Gas Turbine Conditions," *Combustion Science and Technology*, Vol. 87, No. 6, 1993, pp. 329–362.

[4]Davis, D. L., "Coaxial Dump Combustion Instabilities. Part I: Parametric Test Data. Interim Report," Aeropropulsion Lab., Air Force Wright Aeronautical Labs., Wright–Patterson AFB, Ohio.

[5]Logan, P., Lee, J. W., Lee, L. M., and Karagozian, A. R., "Acoustics of a Low Speed Dump Combustor," *Combustion and Flame*, Vol. 84, 1991, pp. 93–109.

[6]Rayleigh, J. W. S., *The Theory of Sound*, Macmillan, New York, 1994, p. 226.

[7]Rogers, D. E., and Marble, F. E., "A Mechanism for High Frequency Oscillations in Ramjet Combustors and Afterburners," *Jet Propulsion*, Vol. 456, June 1956, pp. 456–462.

[8]Yu, K. H., Trouve, A., and Daily, J. W., "Low Frequency Pressure Oscillations in a Model Ramjet Combustor," *Journal of Fluid Mechanics*, Vol. 232, 1991, pp. 47–72.

[9]Smith, D. A., and Zukoski, E. E., "Combustion Instability Sustained by Unsteady Vortex Combustion," AIAA/SAE/ASME/ASEE 21st Joint Propulsion Conf., AIAA Paper 85-1248, 1985.

[10]Poinsot, T. J., Trouve, A. C., Veynante, D. P., Candel, S. M., and Esposito, E. J., "Vortex-Driven Acoustically Coupled Combustion Instabilities," *Journal of Fluid Mechanics*, Vol. 177, April 1987, pp. 265–292.

[11]Schadow, K. C., Gutmark, E., Parr, T. P., Parr, D. M., Wilson, K. J., and Crump, J. E., "Large Scale Coherent Structures as Drivers of Combustion Instability," *Combustion Science and Technology*, Vol. 64, 1989, pp. 167–186.

[12]Schadow, K. C., and Gutmark, E., "Combustion Instability Related to Vortex Shedding and Their Passive Control," *Progress in Energy and Combustion Science*, Vol. 18, No. 2, 1992, pp. 117–132.

[13]Schadow, K. C., Gutmark, E., Wilson, K. J., and Smith, R. A., "Multi-step Dump Combustor Design to Reduce Combustion Instabilities," *Journal of Propulsion and Power*, Vol. 6, No. 4, 1990, pp. 407–411.

[14]Samaniego, J. M., Yip, B., Poinsot, T., and Candel, S., "Low Frequency Combustion Instability Mechanisms in a Side Dump Combustor," *Combustion and Flame*, Vol. 94, No. 4, 1993, pp. 363–380.

[15]Shih, W. P., Lee, J., and Santavicca, D. A., "Stability and Emission Characteristics of a Lean Premixed Gas Turbine Combustor," *Twenty-Sixth (International) Symposium on Combustion*, The Combustion Inst., Pittsburgh, PA, 1996, 2, pp. 2771–2778.

[16]Sivasegaram, S., and Whitelaw, J. H., "Oscillations in Axisymmetric Dump Combustors," *Combustion Science and Technology*, Vol. 52, 1987, pp. 413–426.

[17]Richards, G. A., and Janus, M. C., "Characterization of Oscillations During Premix Gas Turbine Combustion," *Journal of Engineering for Gas Turbines and Power*, Vol. 120, No. 2, 1998, pp. 294–302.

[18]Straub, D. L., and Richards, G. A., "Effects of Fuel Nozzle Configuration on Premix Combustion Dynamics," American Society of Mechanical Engineering, Paper 98-GT-492, June 1998.

[19]Lieuwen, T., and Zinn, B. T., "Theoretical Investigation of Combustion Instability Mechanisms in Lean Premixed Gas Turbines," AIAA Paper 98-0641, Jan. 1998.

[20]Putnam, A. A., *Combustion Driven Oscillations in Industry*, Elsevier, New York, 1974.

[21]Peracchio, A. A., and Proscia, W. M., *Nonlinear Heat-Release/Acoustic Model for Thermoacoustic Instability in Lean Premixed Combustors*, American Society of Mechanical Engineers/International Gas Turbine Institute Turbo Expo, June 1998.

[22]Fleifil, M., Annaswamy, A. M., Ghoneim, Z. A., and Ghoneim, A. F., "Response of a Laminar Premixed Flame to Flow Oscillations: A Kinematic Model and Thermoacoustic Instability Results," *Combustion and Flame*, Vol. 106, Sept. 1996, pp. 487–510.

[23]Beer, J. M., and Chigier, N. A., *Combustion Aerodynamics*, Robert E. Krieger, Malabar, FL, 1983, pp. 100–145.

[24]Lozano, A., Yip, B., and Hanson, R., "Acetone: A Tracer for Concentration Measurements in Gaseous Flows by Planar Laser Induced Fluorescence," *Experiments in Fluids*, Vol. 13, 1992, pp. 369–376.

[25]Hurle, I. R., Price, R. B., Sugden, T. M., Thomas, F. R. S., and Thomas, A., "Sound Emission from Open Turbulent Premixed Flames," *Proceedings of the Royal Society of London*, Vol. 303, 1968, pp. 409–427.

[26]Samaniego, J. M., Egolfopoulos, F. N., and Bowman, C. T., "CO_2^* Chemiluminescence in Premixed Flames," *Combustion Science and Technology*, Vol. 109, 1995, pp. 183–203.

[27]Bandaru, R. V., Miller, S., Lee, J., and Santavicca, D. A., "Sensors for Measuring Primary Zone Equivalence Ratio in Gas Turbine Combustors," *Proceedings of SPIE*, International Society for Optical Engineering, Bellingham, Washington, Vol. 3535, 1998, pp. 104–114.

[28]Najm, H. N., Paul, P. H., Mueller, C. J., and Wyckoff, P. S., "On the Adequacy of Certain Experimental Observables as Measurements of Flame Burning Rate," *Combustion and Flame*, Vol. 113, 1998, pp. 312–332.

[29]Law, C. K., "Dynamics of Stretched Flames," *Twenty-Second (International) Symposium on Combustion*, The Combustion Inst., Pittsburgh, PA, 1988, pp. 1381–1402.

[30]Lee, J. G., Lee, T.-W., Nye, D. A., and Santavicca, D. A., "Lewis Number Effects on Premixed Flames Interacting with Turbulent Karman Vortex Streets," *Combustion and Flame*, Vol. 100, No. 1–2, 1995, pp. 161–168.

[31]Darabhia, N., Candel, S. M., Giovangigli, V., and Smooke, M. D., "Extinction of Strained Premixed Propane–Air Flames with Complex Chemistry," *Combustion Science and Technology*, Vol. 60, 1988, pp. 267–285.

[32]Dasch, C. J., "One-Dimensional Tomography: A Comparison of Abel, Onion-Peeling and Filtered Back Projection Methods," *Applied Optics*, Vol. 31, No. 8, 1992, pp. 1146–1152.

[33]Turns, S. R., *An Introduction to Combustion*, McGraw–Hill, New York, 1996, pp. 224–232.

[34]Katsuki, M., and Whitelaw, J. H., "The Influence of Duct Geometry on Unsteady Premixed Flames," *Combustion and Flame*, Vol. 63, 1986, pp. 87–94.

[35]Langhorne, P. J., "Reheat Buzz: An Acoustically Coupled Combustion Instability. Part 1—Experiment," *Journal of Fluid Mechanics*, Vol. 193, 1988, pp. 417–443.

[36]Keller, J. O., and Saito, K., "Measurements of the Combusting Flow in a Pulse Combustor," *Combustion Science and Technology*, Vol. 53, 1987, pp. 137–163.

[37]Fernandes, E. C., and Heitor, M. V., "Unsteady Flames and the Rayleigh Criterion," *Unsteady Combustion*, NATO ASI Series, 1993, pp. 1–16.

[38]Reuter, D. M., Hegde, U. G., and Zinn, B. T., "Flowfield Measurements in an Unstable Ramjet Burner," *Journal of Propulsion and Power*, Vol. 6, No. 6, 1990, pp. 680–685.

[39]Lieuwen, T., Neumeier, Y., and Zinn, B. T., "Role of Unmixedness and Chemical Kinetics in Driving Combustion Instabilities in Lean Premixed Combustors," *Combustion Science and Technology*, Vol. 135, No. 1–6, 1998, pp. 193–211.

[40]Ahmed, S. A., and Nejad, A. S., "Swirl Effects on Confined Flows in Axisymmetric Geometries," *Journal of Propulsion and Power*, Vol. 8, No. 2, 1992, pp. 339–345.

[41]Sivasegaram, S., and Whitelaw, J. H., "The Influence of Swirl on Oscillations in Ducted Premixed Flames," *Combustion and Flame*, Vol. 85, 1991, pp. 195–205.

[42]Seo, S., "Parametric Study of Lean Premixed Combustion Instability in a Pressurized Model Gas Turbine Combustor," Ph.D. Thesis, Dept. of Mechanical and Nuclear Engineering, Pennsylvania State Univ., May 1999.